Available online at www.sciencedirect.com
ScienceDirect
Trans. Nonferrous Met. Soc. China 33(2023) 701−713
Transactions of Nonferrous Metals Society of China
www.tnmsc.cn

Effect of annealing temperature on microstructure and tensile properties of copper/aluminum composite thin strip

Chen WANG[1,2,3], Li-nan MA[4], Xiao-guang MA[1,2,3], Tao WANG[1,2,3],
Zheng-yi JIANG[5,6], Mahadi HASAN[7], Jing-wei ZHAO[1,2,3]

1. College of Mechanical and Vehicle Engineering, Taiyuan University of Technology, Taiyuan 030024, China;
2. Engineering Research Center of Advanced Metal Composites Forming Technology and Equipment, Ministry of Education, Taiyuan 030024, China;
3. TYUT-UOW Joint Research Center, Taiyuan University of Technology, Taiyuan 030024, China;
4. School of Mechanical Engineering, Taiyuan University of Science and Technology, Taiyuan 030024, China;
5. School of Mechanical, Materials, Biomedical and Mechatronic Engineering, University of Wollongong, NSW 2522, Australia;
6. TYUT-UOW Joint Research Center, University of Wollongong, NSW 2522, Australia;
7. Department of Industrial and Production Engineering, American International University Bangladesh, Dhaka 1229, Bangladesh

Received 29 October 2021; accepted 20 February 2022

Abstract: The effect of annealing temperature on the microstructure and tensile properties of copper/aluminum (Cu/Al) composite thin strips was studied to improve the mechanical properties of materials. The change of interface layer, the diffusion of interface elements, and the microstructural evolution of each matrix of Cu and Al were observed and analyzed using scanning electron microscope (SEM), energy dispersive spectroscopy (EDS) and electron back-scatter diffraction (EBSD) techniques. The tensile properties of the Cu/Al composite thin strip were studied by static uniaxial tensile tests. The results show that recrystallization occurs in the Cu/Al matrix during annealing process, and the grains of the Al matrix grow into coarse grains after annealing at 400 °C. The thickness of diffusion layer increases with the increase of annealing temperature, and the thickness of the diffusion layer reaches 12 μm after annealing at 500 °C. The original typical rolling texture is transformed into the typical annealing texture components {001}⟨100⟩ and {001}⟨110⟩ after annealing treatment. In general, the annealing treatment reduces the tensile strength and improves the overall plasticity of the material, and the diffusion layer plays a significant role in transmitting tensile stress.
Key words: copper/aluminum composite; annealing; microstructure; texture; tensile properties

1 Introduction

Metallic laminated composites are attracting increasing attention in recent years with combining the mechanical, physical and chemical properties of dissimilar materials. With the advantages of high strength, high formability, effective corrosion resistance as well as excellent electrical and thermal conductivity, copper/aluminum (Cu/Al) composite thin strip is widely used in a variety of fields such as automobile and electronic industry [1].

Cu/Al composites can be obtained through several processing techniques including roll-bonding [2−6], explosive welding [7], friction stir welding [8,9], hot-pressed diffusion [10], spark plasma sintering [11], and cold-drawing [12]. Among these methods, roll-bonding is mainly used for the production of laminated composites, owing to the characteristics of the low cost and high

Corresponding author: Jing-wei ZHAO, E-mail: jzhao@tyut.edu.cn
DOI: 10.1016/S1003-6326(22)66139-9

efficiency [4]. In order to meet the demands of excellent mechanical properties, composites are usually underwent heat treatment to relieve the processing stress on the surface and internal layer of the materials, thereby optimizing the microstructure and improving the mechanical properties of the composites [13]. The development of the phases at the interface of roll-bonded Cu/Al composites significantly affects the strength [2]. Based on previous studies [5,14−18], a large amount of energy promotes the diffusion between Cu and Al matrixes during annealing process. For the mechanical point of view, the generation of complex Cu−Al intermetallic compounds (IMCs), including $CuAl_2$, CuAl and Cu_9Al_4, at the interface reduces the overall ductility, and these IMCs give additional hardening to the interface. After cold-roll bonding, the appearance of IMCs strengthens the bonding strength between Cu and Al matrixes, while thicker IMCs layers promote the crack propagating and deteriorate bonding.

HENESS et al [2] found that initial rolling reduction appeared to have no effect on phase development, and fracture occurred in the hard and brittle Cu-rich phase [4]. Inspection of the fracture surface showed that the fracture originated from brittle IMCs, and the fracture in the Cu/Al composites was of ductile type. LI et al [19,20] conducted a relatively systematic research on the Cu/Al composites produced by asymmetric roll-bonding, and found that asymmetric roll-bonding provided a remarkable cross shear, and promoted the surface to deform and extend. With large mismatch speed ratio, the interface bonded tightly. The laminated Cu/Al composites were fabricated by means of cold rolling [5,6,18,21] and explosive-welding [7], and heat treatment with different temperatures and soaking time was conducted to investigate the Cu/Al interface structure and bonding strength. The results showed that heat treatment with low temperature and short soaking time could improve the bonding strength of the Cu/Al/Cu laminates significantly [18]. KIM and HONG [21,22] investigated the bending behavior and fracture phenomenon of Cu/Al composite, and found that fatal crack perpendicular to the Cu/Al interface through the Cu layer was formed by large tensile stress. TAYYEBI et al [23] found that the tensile strength of Cu/Al multilayered composite processed by accumulative roll bonding reached 566.5 MPa, and the tensile strength of the annealed specimens showed a declining trend at lower annealing temperatures and time while an increase at higher conditions.

In the current work, Cu/Al composite thin strip fabricated by semi-molten cast-rolling processes was annealed at different temperatures, and a series of tensile tests were performed to study the effect of annealing temperature on the tensile properties. By analyzing the mechanism of the formation of IMCs during the annealing process, the interface microstructure and its influence on the mechanical properties were studied. The grain orientation, grain boundary and texture in the Cu and Al matrixes were characterized, and their effects on the mechanical properties of the composites were discussed. This work aims to study the growth law of IMCs and the evolution of microstructure and texture of the Cu and Al matrixes, and to improve the mechanical properties and formability of Cu/Al composite thin strip.

2 Experimental

Commercial Cu/Al composite thin strip (0.6 mm total thickness) composed of a 75 μm-thick pure copper T2 layer and a 525 μm-thick aluminum 1060 layer was employed as experimental material, and its chemical compositions are given in Table 1. In order to investigate the effect of annealing temperature on the mechanical properties and microstructure, the as-received composite strip was annealed at 300, 400 and 500 °C, respectively, for 1 h. The as-received specimen is named as A0, and the specimens annealed at 300, 400 and 500 °C are named as A300, A400 and A500, respectively. The entire annealing process was carried out in a tubular vacuum heating furnace, and argon gas was introduced for protection during the annealing period. The microstructure of the specimens was investigated using scanning electron microscope (SEM), energy dispersive spectroscopy (EDS) and electron back-scatter diffraction (EBSD) techniques.

Table 1 Chemical composition of as-received Cu/Al composite thin strip (wt.%)

Material	Cu	Al	Fe	S	Sn	Si	Ti
Cu (T2)	99.9	−	0.008	0.005	0.008	−	−
Al (1060)	−	99.61	0.26	−	−	0.08	0.013

Tensile specimens (see Fig. 1) were wire cut according to the ASTM E8M standard [24] along the rolling direction (RD), and the tests were conducted using an Instron Series 5969 universal tensile testing machine at room temperature with a strain rate of 3.3×10^{-4} s^{-1}. The fracture surfaces of tensile specimens were observed by SEM.

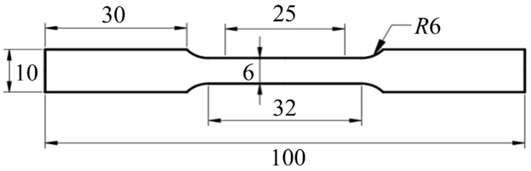

Fig. 1 Dimensions of specimen used for tensile test (unit: mm)

The cross sections of the as-received and annealed specimens were prepared for micro-structural observation and texture analysis. EBSD tests were performed using a JOE IT500 SEM which was equipped with an Oxford HKL channel 5 software. The crystallographic orientation of grains in the scanned area was obtained with a step size of 0.1 μm. Additionally, the average grain size of Cu and Al matrixes was obtained based on statistic results from EBSD maps. In order to study the correlation between texture and tensile properties of Cu/Al composite thin strip, the texture components were further analyzed based on the orientation distribution functions (ODFs).

3 Results

3.1 Interfacial structure

Figure 2 shows the SEM images of interface and EDS line scanning spectra of the specimens annealed at different temperatures. As shown in Fig. 2(a), a significant diffusion layer is formed at the interface of the Specimen A0. A short plateau can be found on the elemental distribution curves of Cu and Al obtained from EDS. The total thickness of the IMCs layers is approximately 3 μm. Figure 2(b) shows the interface of the Specimen A300, and it is found that the thickness of the diffusion layer does not increase significantly, while the IMC layer grows along the RD compared to the Specimen A0. Also, the distribution of the diffusion layer is discontinuous, and the thickness is uneven, indicating that the IMCs do not get enough energy for growth at 300 °C. For the Specimen A400 as shown in Fig. 2(c), obvious interfacial IMCs layer comprising three sublayers is formed with the overall average thickness of 5 μm, and the diffusion layer is found to be of uniform thickness and continuous distribution. Also, the curves of Cu and Al content show a slow linear change. From

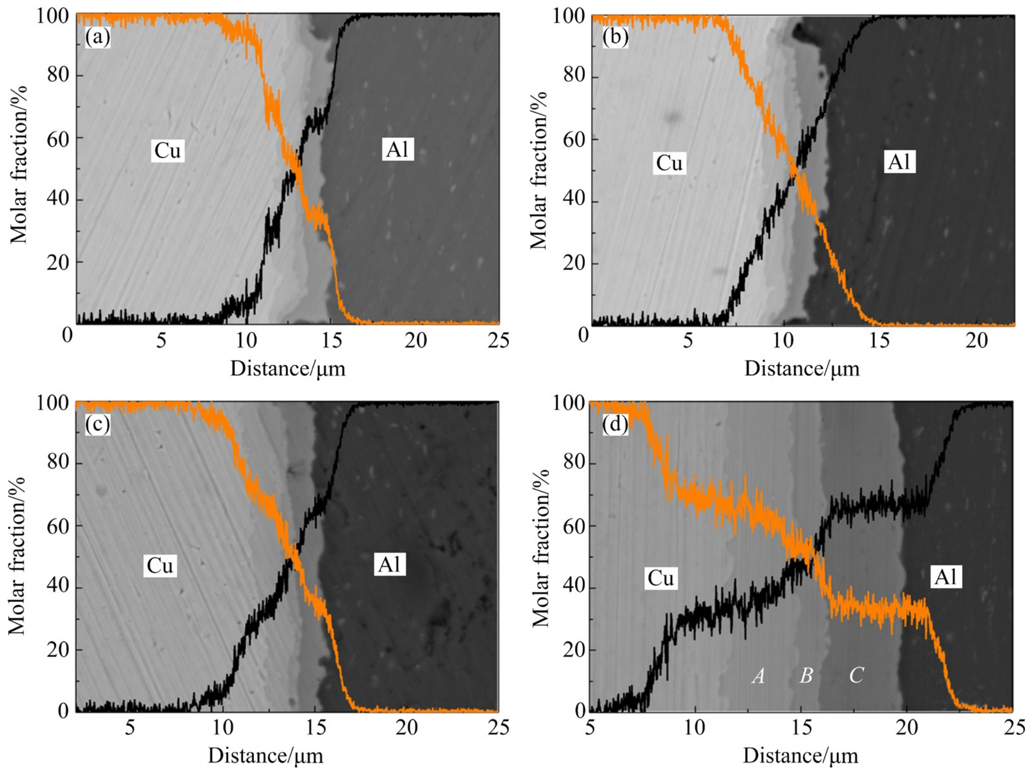

Fig. 2 SEM images and EDS line scanning spectra of specimens: (a) A0; (b) A300; (c) A400; (d) A500

Fig. 2(d), it can be seen that the diffusion layer grows rapidly along the thickness direction, and the total thickness reaches 12 μm after annealing at 500 °C. The results of EDS point analysis in Fig. 2(d) are as follows: 52.3 Cu and 23.3 Al (in at.%) for Point *A*, 40.1 Cu and 38.7 Al (in at.%) for Point *B*, and 24.3 Cu and 51.4 Al (in at.%) for Point *C*, respectively, which further identify the sublayer adjacent to Cu matrix as Cu_9Al_4 phase, the middle layer as CuAl phase, and the thick layer adjacent to Al matrix as $CuAl_2$ phase, which are consistent with the previous reports [12,14,15]. Figure 3 displays the phase distribution of the interface of the Specimen A400 by EBSD technique. There are five phases near the interface, which are Al, $CuAl_2$, CuAl, Cu_9Al_4 and Cu, respectively, from Al to Cu side.

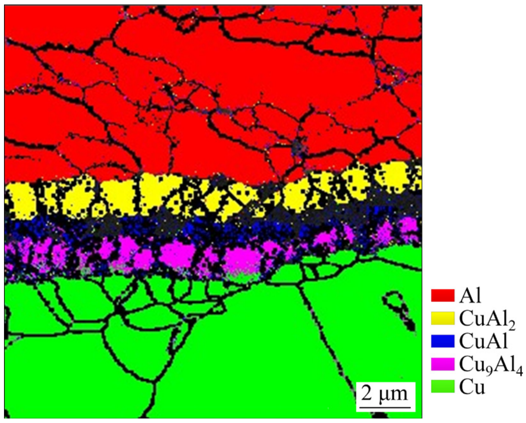

Fig. 3 Phase distribution of Specimen A400

3.2 Microstructure

Figure 4 shows the inverse pole figure (IPF) maps of Specimens A0, A300, A400 and A500,

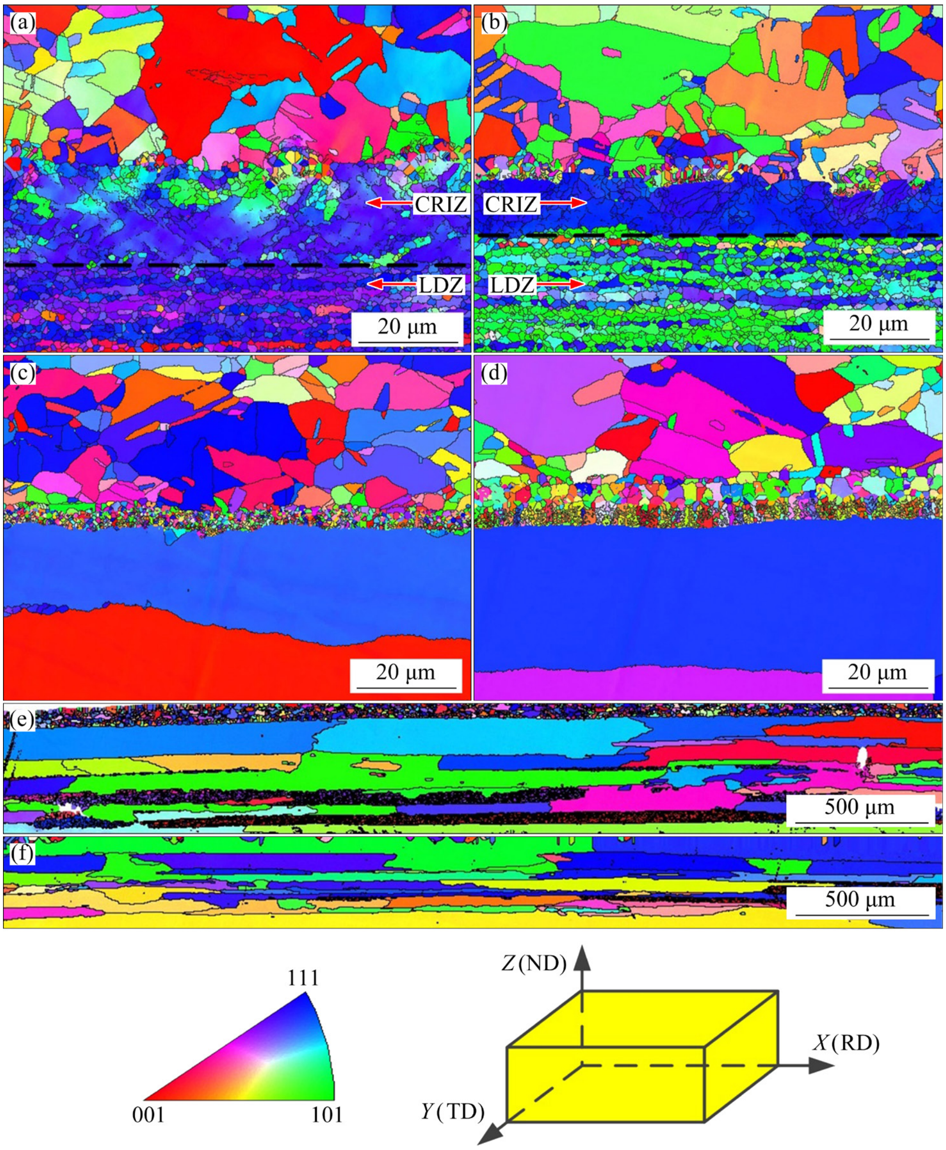

Fig. 4 IPF maps of Specimens A0 (a), A300 (b), A400 (c) and A500 (d), and amplification for A400 (e) and A500 (f)

respectively, from which three band-shaped regions, namely the Cu matrix, the interface, and the Al matrix can be clearly observed. The average grain sizes in the Cu matrix are 3.75, 3.59, 3.64 and 4.11 μm for the Specimens A0, A300, A400 and A500, respectively. In addition, a small amount of twins can be observed inside the Cu matrix. It is known that Cu has a typical face-centered cubic (FCC) crystalline structure and its stacking fault energy is relatively low, so the atoms are prone to misalignment and form twins during the recrystallization process [14]. In the present work, the Al matrix is divided into the cast-rolling near-interface zone (CRIZ) and the large deformation zone (LDZ). The average grain sizes in the CRIZ and LDZ for the Specimen A0 are 2.83 and 2.26 μm respectively (Fig. 4(a)). After annealing at 300 °C, the CRIZ is replaced by recrystallized grains and the thickness of it is reduced below 20 μm, as shown in Fig. 4(b). However, no complete grains can be photographed under the same magnification for the Specimens A400 and A500, as shown in Figs. 4(c) and (d). This can be attributed to the remarkable growth of Al grains for the Specimens A400 and A500, and the slender fibrous coarse grains are observed clearly, as shown in Figs. 4(e) and (f).

Figure 5 shows the distribution of low-angle

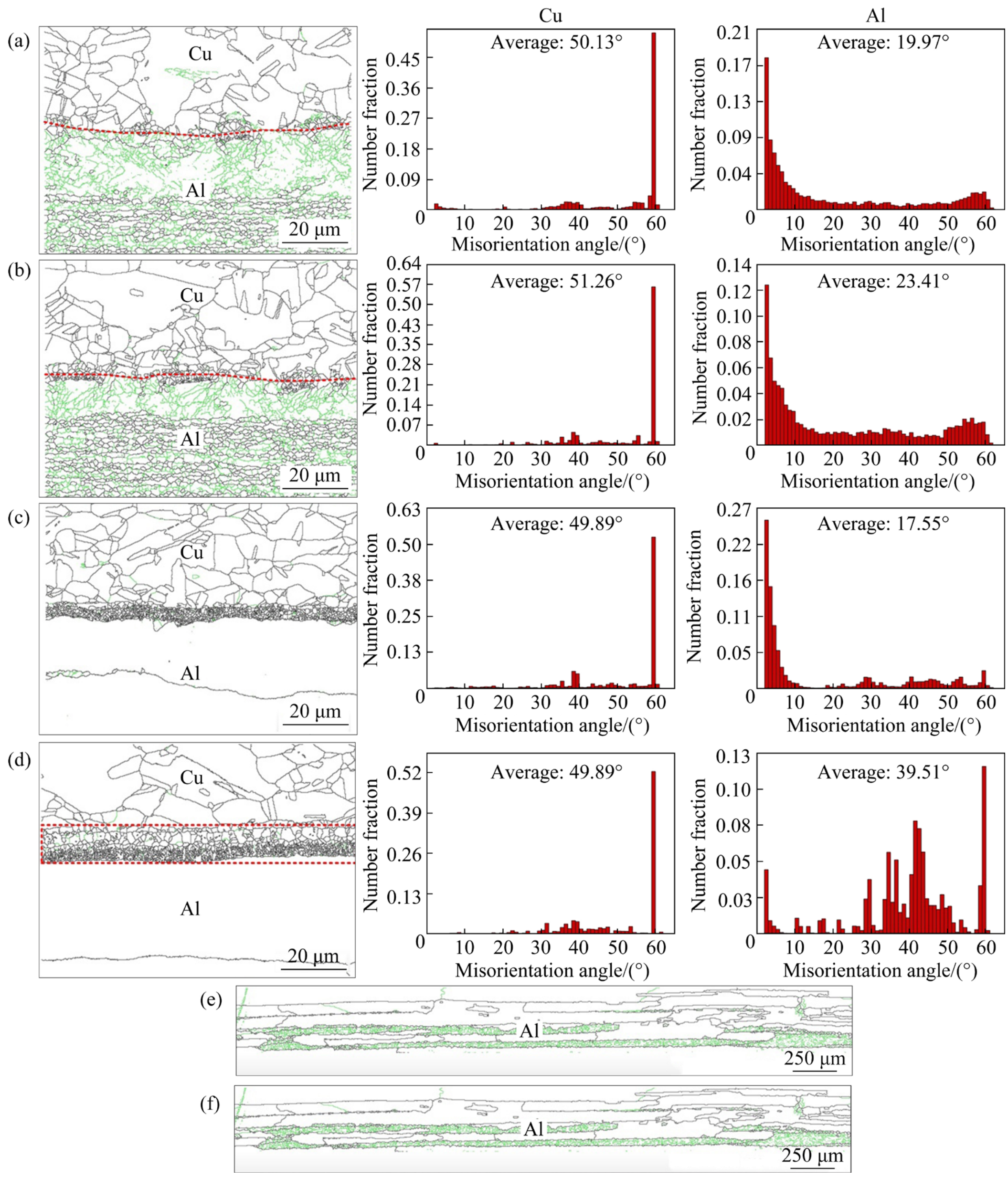

Fig. 5 Cross-sectional EBSD images showing low-angle (2°−15°, green) and high-angle (>15°, black) grain boundaries with grain boundary misorientations of Al and Cu: (a) A0; (b) A300; (c) A400; (d) A500; (e) Amplification for A400; (f) Amplification for A500

(2°−15°, green) and high-angle (>15°, black) grain boundaries in the Specimens A0, A300, A400 and A500, respectively. The average grain boundary misorientation angle in the Cu matrix is found to fluctuate at around 50°. Additionally, there is a peak at 60° in the distribution diagrams of Cu matrix, confirming the existence of an amount of twin boundaries. On the other hand, the low-angle grain boundaries are mainly distributed in the near-interface zone of the Al matrix for the Specimen A0. The average grain boundary misorientation angle increases from 19.97° to 23.41° after annealing at 300 ℃, with the area of CRIZ zone decreasing and that of LDZ increasing. For the Specimen A400, as the grains on the Al side grow, low-angle grain boundaries appear inside the coarse grains, and the average grain boundary misorientation angle is reduced to 17.55°. As the annealing temperature increases to 500 ℃, a remarkable increase of the average grain boundary misorientation angle is observed from 17.55° to 39.41°, which can be attributed to the increased energy absorption by the Al side matrix [25].

3.3 Texture

The ODF sections of Cu and Al matrixes annealed at different temperatures are shown in Figs. 6 and 7, respectively. The diagrams are from the cross sections with φ_2=0° and φ_2=45°, which are capable of comprehensively reflecting the grain orientation distribution and most texture components of Cu/Al composite thin strip. Figure 8 shows the scheme of the ideal texture components for ODFs. In the Cu matrix of the Specimen A0, the ODF displays strong {025}⟨100⟩ component, with the maximum intensity of 47.8. In addition, as the annealing temperature increases, the intensity of the {025}⟨100⟩ component decreases. At the

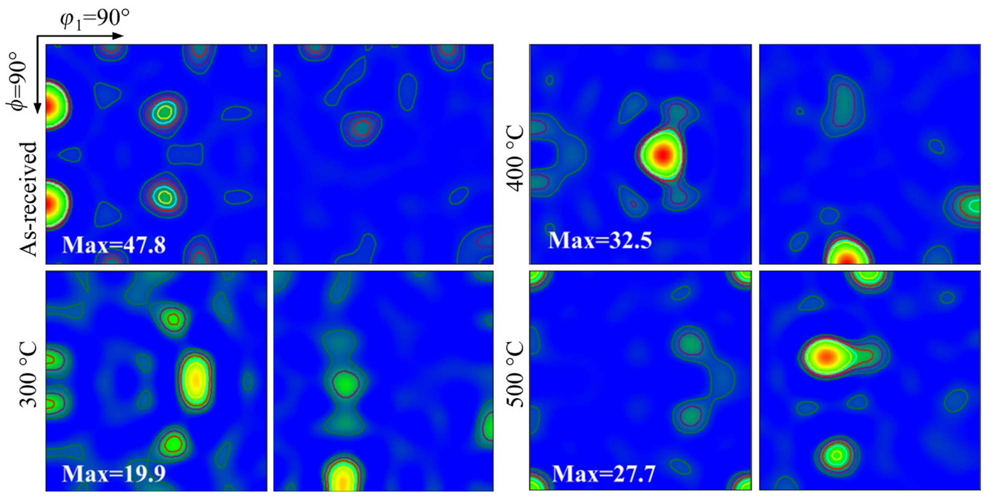

Fig. 6 ODF diagrams of Cu matrix annealed at different temperatures

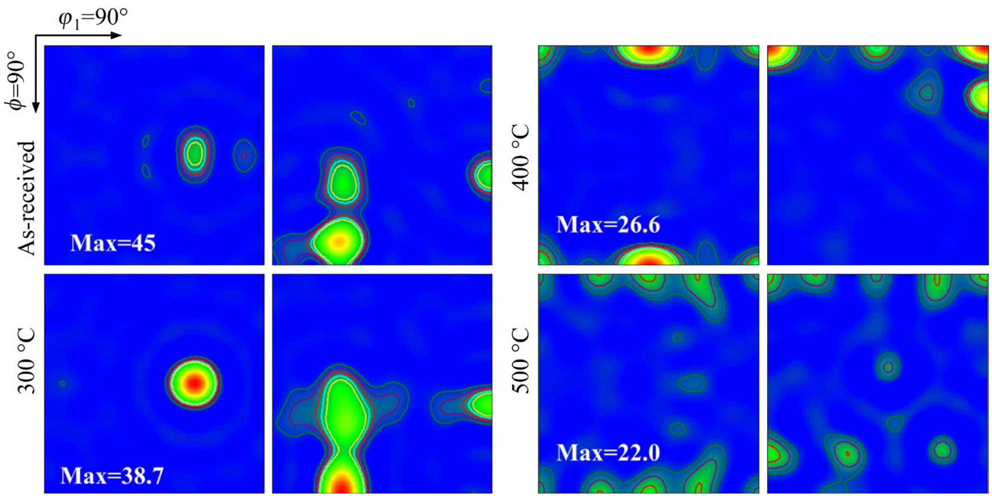

Fig. 7 ODF diagrams of Al matrix annealed at different temperatures

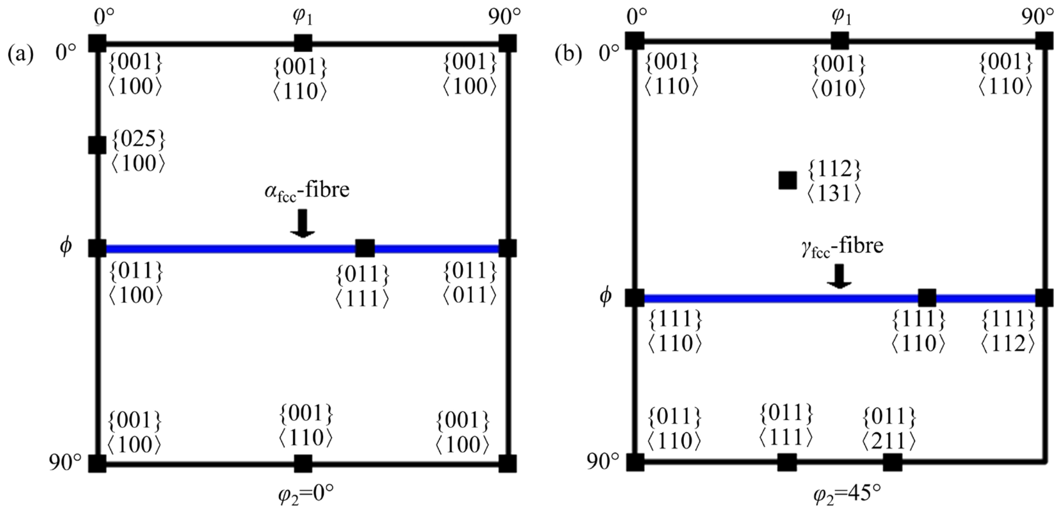

Fig. 8 Ideal texture components for ODF sections: (a) φ_2=0°; (b) φ_2=45°

same time, the {011}⟨111⟩ α_{fcc}-fiber and {111}⟨112⟩ components begin to form inside the specimen after annealing at 300 °C and become stronger when the annealing temperature increases to 400 °C, with the maximum intensity increasing from 19.9 to 32.5. While after annealing at 500 °C, it is found that the {011}⟨111⟩ α_{fcc}-fiber component is gradually transformed into the {112}⟨131⟩ component, and the maximum intensity becomes 27.7, also with the weak {001}⟨100⟩ component.

The part of Al matrix in the Specimen A0 contains the {011}⟨111⟩ α_{fcc}-fiber and {111}⟨112⟩ components, with the maximum intensity reaching 45. For the Specimen A300, the maximum intensity decreases to 38.7. Additionally, the {011}⟨111⟩ α_{fcc}-fiber component is strengthened, and the {001}⟨110⟩ and {001}⟨100⟩ components form with the maximum intensity rising to 26.6 after annealing at 400 °C. For the Specimen A500, the intensity of major texture components decreases.

3.4 Tensile properties and fractograph

Figure 9 shows the engineering stress−strain curves of the Specimens A0, A300, A400 and A500. It can be seen that the ultimate tensile strength of the Specimen A300 is slightly lower than that of the Specimen A0. With the increase of annealing temperature from 300 to 500 °C, dramatic decrease of tensile strength can be observed, while the elongation greatly increases from 17.1% to 23.6%.

Figure 10 presents the fracture surfaces of the tensile specimens. It is clear that the fracture morphology of all the specimens is relatively flat, and there is obvious shrinking at the far interface of the Cu and Al sides. Since Al exhibits better plasticity than Cu, the shrinking on the Al side is more obvious. In addition, with the increase of annealing temperature, the cracks of the interface fracture become wider and deeper, and the amount of dimples increases a lot on the fracture surface, especially for the specimens annealed at 500 °C. When the observation magnification is increased, IMCs have been clearly observed in the fracture cracks, and the thickness is found to increase significantly with the increase of annealing temperature.

4 Discussion

4.1 Evolution of interface phase structure

The two metal components of Cu and Al are very easy to form IMCs due to the diffusion reaction during the annealing process [4], and they will have a non-negligible effect on the bonding strength and the tensile coordinated deformation behavior of the composite strip [26]. It is known that Cu atom has a smaller diameter (d_{Cu}=0.1278 nm) than that of Al atom (d_{Al}=0.1432 nm) [11], and the diffusion rate of Cu in Al (9.2×10^{-5} $m^2\cdot s^{-1}$) is higher than that of Al in Cu (3.4×10^{-6} $m^2\cdot s^{-1}$) at 110 °C, consequently Cu atoms can diffuse into the Al side rapidly [13]. Also, $CuAl_2$ has the lowest effective heat of formation among several IMCs ($CuAl_2$: 6.1 $kJ\cdot mol^{-1}$, CuAl: 5.1 $kJ\cdot mol^{-1}$ and Cu_9Al_4: 4.1 $kJ\cdot mol^{-1}$) [14]. The effective heat of formation model explains the appearance of $CuAl_2$ as the first phase in the diffusion zone. However, there are diverse views on the formation sequence of the next

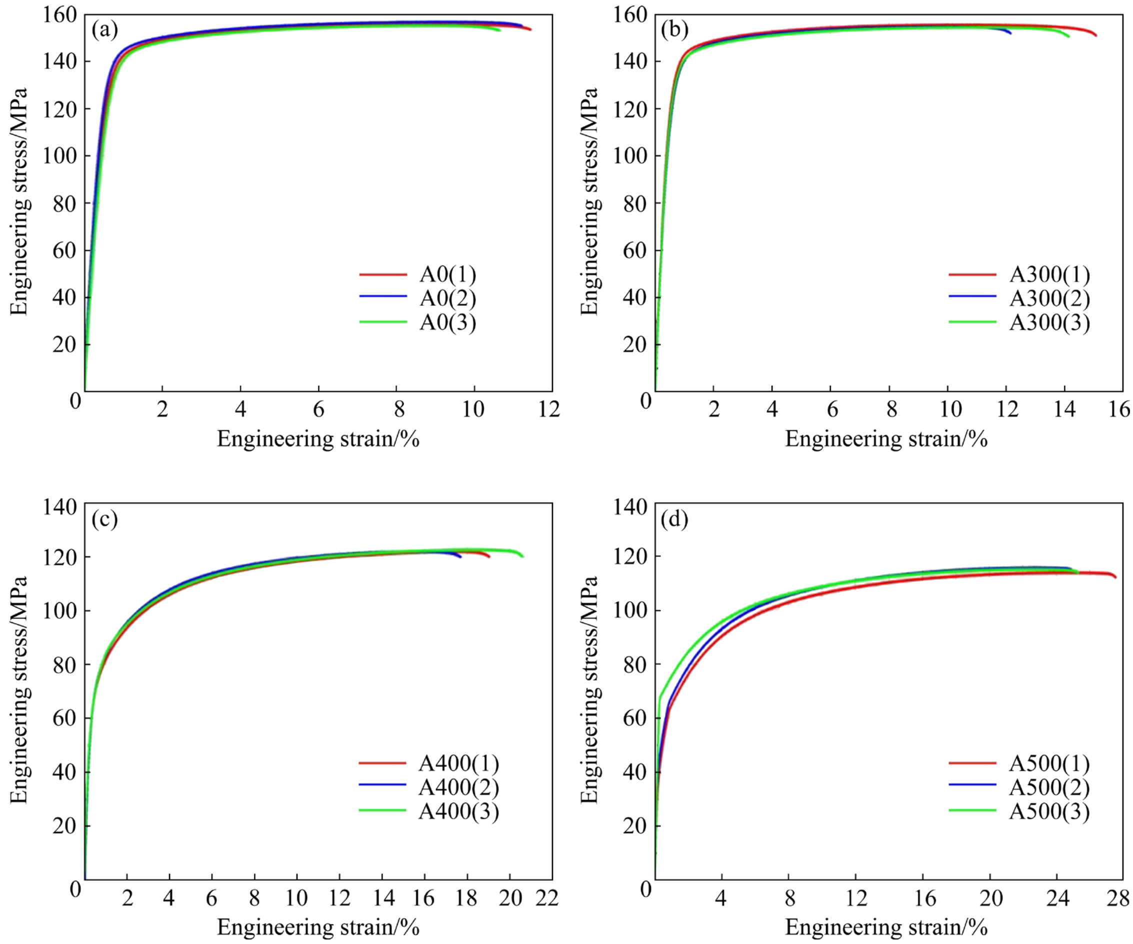

Fig. 9 Stress−strain curves of tensile specimens: (a) A0; (b) A300; (c) A400; (d) A500

IMCs CuAl and Cu_9Al_4. XU et al [14] found that Cu_9Al_4 formed prior to CuAl, indicating that kinetics, rather than thermodynamics, was dominant during the annealing process. The formation of Cu_9Al_4 in preference to CuAl can be attributed to the high driving force for formation.

The evolution of the interfacial microstructure and phase formation process in Cu/Al thin strips are illustrated in Fig. 11. IMCs are first formed due to a large amount of local element diffusion and aggregation. According to the classical kinetic theory, growth rate constant D is characterized by the temperature and activation energy, as given by the Arrhenius equation:

$$D = D_0 \exp\left(-\frac{Q}{RT}\right) \tag{1}$$

where D_0 is the pre-exponential factor, Q is the growth activation energy, R is the mole gas constant, and T is the thermodynamic temperature.

For the same IMC, as the annealing temperature increases, the diffusion reaction rate will increase significantly. Therefore, the atoms near the interface will gain more energy at higher temperature when the holding time is the same, making the diffusion reaction more violent. Additionally, with the increase of annealing temperature, an increase of the thickness of the uniformly distributed diffusion layer can be observed as shown in Fig. 10, which demonstrates the changes of IMCs during annealing process at different temperatures. Combining Figs. 2 and 10, the contact of molten Al with Cu strip leads to heat exchange during casting rolling process, especially at the interface, the high temperature activates the diffusion movement of Cu and Al atoms [17]. The heat generated by rolling friction promotes the solid solution saturation and further formation of IMCs [10]. Additionally, as the composite strip undergoes plastic deformation, the slip bands and dislocations near the interface provide channels for atomic diffusion. Thus, solid solutions are formed at the local defect positions of the interface.

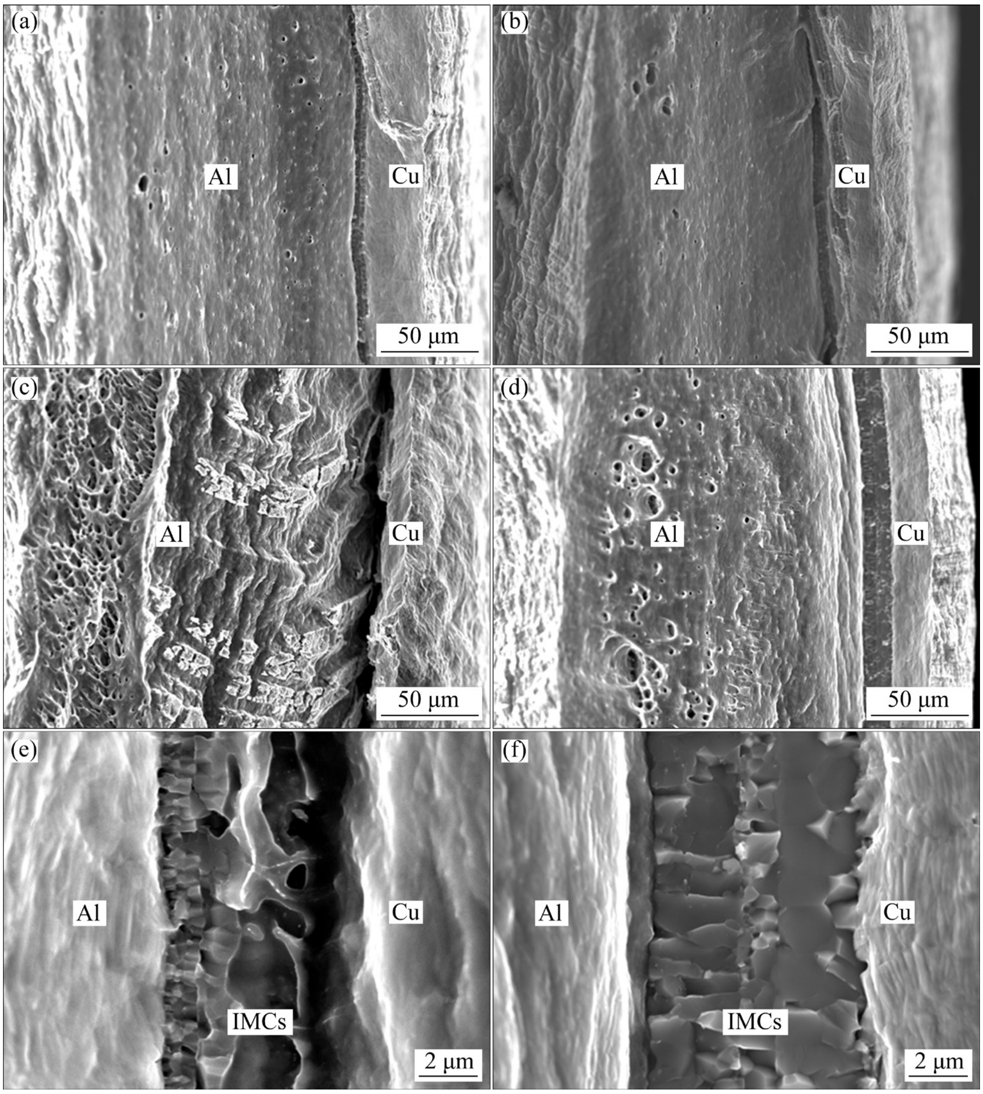

Fig. 10 Fracture surfaces of tensile specimens: (a) A0; (b) A300; (c) A400; (d) A500; (e) IMCs in Specimen A400; (f) IMCs in Specimen A500

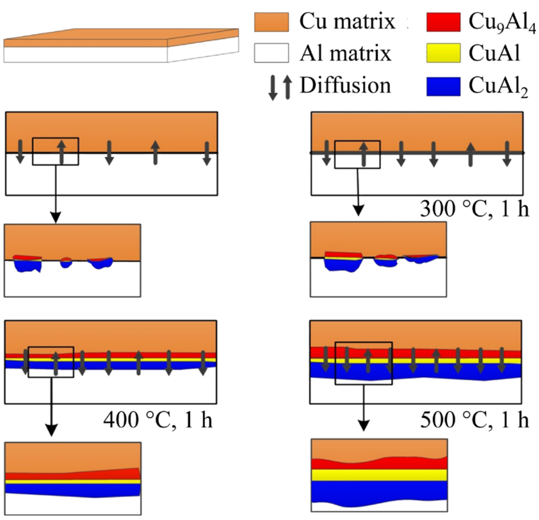

Fig. 11 Schematic diagram of IMCs formation at Cu/Al interface during annealing

According to the research by XU et al [14], IMCs exhibit high strength, but low ductility. In addition, IMCs have a large lattice difference with Al and Cu crystals. Different mechanisms of interface types make it difficult for dislocations to pass through the interface [15], resulting in high stresses along the interface [18]. As the Al layer exhibits better plasticity than that of Cu layer, plastic deformation will occur earlier on the Al layer under tensile loading. However, under the retarding of the harder Cu layer, dislocation slip in the Al matrix cannot be fully activated, and it will accumulate near the interface. Due to the hard and brittle characteristics of IMCs, more serious dislocation blockage and accumulation will occur around the Al grain boundaries bordering IMCs, which produces a long-range back stress that makes the dislocation slip in the Al matrix more difficult [16]. As a consequence, only slight decrease of tensile strength can be observed on the specimens annealed at 300 °C (Fig. 9). With the annealing temperature increasing, the thickness of IMCs also increases, so that this effect is greatly weakened. Thus, dramatic decrease in the tensile strength of the specimens annealed at 400 and 500 °C is observed.

4.2 Evolution of matrix microstructure

4.2.1 Grain structure

Cu has a FCC crystal structure, and has a stacking fault energy lower than 100 mJ·m^{-2}. As a result, annealing twins form primarily in FCC materials that have low stacking fault energy [27], which plays a significant role in the plastic deformation of materials. Also, it is indicated that the recrystallization fraction in Cu is higher than that in Al (Fig. 12). The recrystallization fraction in Cu increases intensively from 18.8% to 83.8% after annealing at 300 °C, and the recrystallization fraction further increases beyond 90% when annealing at 400 and 500 °C. The variation of the average grain size indicates that the Cu matrix undergoes nucleation during the annealing process at 300 °C. For the specimens annealed at higher annealing temperatures, the grains grew compared to that of the as-received specimen. On the other hand, a large number of low-angle grain boundaries are found in the Al matrix for the as-received specimen and that annealed at 300 °C. The low-angle grain boundaries are formed by dislocations [28], so most of the A1 region is occupied by low-angle grain boundaries. In this research, the Al matrix is divided into CRIZ and LDZ. There are two main sources of dislocations in the CRIZ [9,12]: (1) during the solidification of molten Al, the crystals will meet when they nucleate and grow, and dislocations are formed due to the crystal orientations; (2) during the rolling processes, the solidification speed of Al surface and Al near the interface are different, and a shear band is formed between the solid Al and the semi-solid Al, which also promotes the formation of dislocations. As for the LDZ, the main reason is that the solid Al undergoes severe plastic deformation during rolling processes, consequently the density of dislocations will increase as the degree of deformation increases [17].

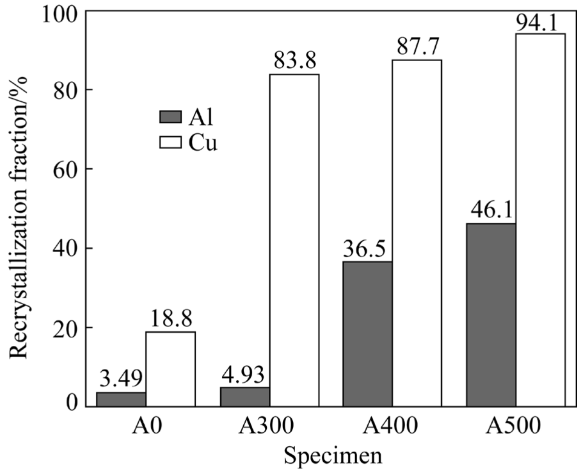

Fig. 12 Recrystallization fraction of Specimens A0, A300, A400 and A500

In the LDZ of the Al matrix, a large number of approximately equiaxed grains can be observed, and the surrounding grain boundaries are mostly high-angle grain boundaries, as shown in Figs. 4 and 5. These phenomena directly indicate the existence of internal dislocations of crystal grains and the process of low-angle grain boundaries annihilation to form high-angle grain boundaries, which suggests that recovery has occurred during annealing treatment [29]. When the annealing temperature reaches 400 °C, recrystallization has completed and the grains continue to grow, and further the grain size in the Al matrix at 500 °C becomes coarse. Considering the decrease of ultimate tensile strength, the grain size can be roughly estimated using the Hall−Petch relationship that the tensile strength is inversely proportional to the square root of grain size [30]. As the grain size decreases, the proportion of grain boundaries in the microstructure increases remarkably, which causes more dislocation accumulations around the grain boundaries. Consequently, higher stress is required to activate the dislocations in adjacent crystals, leading to the increase of the strength of the materials [31]. Therefore, when the crystal grains in the Al matrix grow up, it is more conductive to the development of dislocations, and a decrease of the strength and an increase of elongation are observed.

The Schmid's law gives the relationship among external load, crystal orientation and critical slitting stress as [32]

$$\mu=\cos\phi\cos\lambda=\tau_c/\sigma_s \tag{2}$$

where μ is the tensile deformation orientation factor, ϕ is the angle between tensile direction and normal direction of slip plane, λ is the angle between tensile direction and slip direction, τ_c is the critical resolved shear stress, and σ_s is the yield strength.

In Fig. 13(a), the direction l in the figure is the tensile load direction, and the orientation factor depends on the cosine value of the tensile direction in the normal direction n of the slip plane and the slip direction b. Figure 13(b) shows the distribution of orientation factors calculated by Eq. (2) on different crystal phases when the single system of FCC metal ({111}⟨110⟩ slip system) starts and causes plastic deformation.

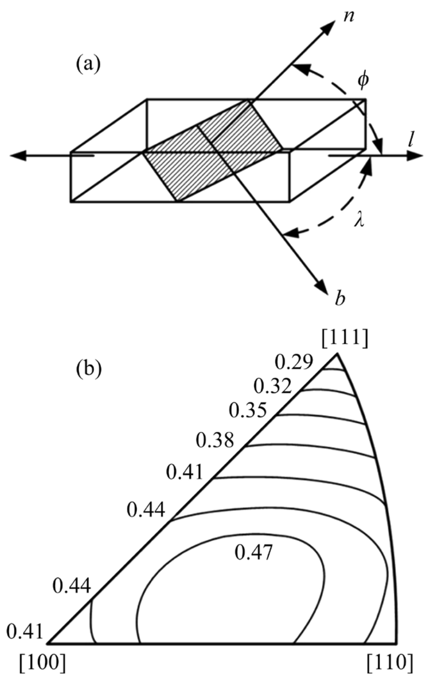

Fig. 13 Force analysis of slip system (a) and IPF of orientation factor μ value (b)

Combined with the grain orientation information in the IPF in Fig. 4, in the as-received specimen, the grain orientations in the Al matrix are mostly concentrated in the ⟨111⟩ direction. According to the orientation factor distribution map, the μ value along the ⟨111⟩ direction is the lowest, which means that it is difficult to slip along this orientation. The orientations of nearly 2/3 of the grains in the Al matrix in the specimen subjected to heat treatment at 300 °C are concentrated in the ⟨101⟩ direction, and the nearby μ value is higher, which is the soft orientation zone. This is also one of the reasons why the tensile strength of the thin strip is reduced.

4.2.2 Texture

Texture evolution is an important aspect of the study of material thermal stability. It directly affects the anisotropy of the mechanical behavior of the structure after annealing, thereby affecting the strength and plasticity of the material. EBSD results are provided to study the effect of annealing temperature on the texture evolution of the Cu/Al composite strip. Given that the thickness of the Cu matrix in the composite strip is small, the impact of Cu matrix on the overall mechanical properties of the material, therefore, is less than that of Al matrix. The research on Cu is more inclined to the evolution of texture under the rolled and annealed states. Based on the analysis of Figs. 4 and 6, the grain orientation of Cu matrix under the initial state is strongly anisotropic, and the high-intensity {025}⟨100⟩ component is formed locally, which belongs to the β-fiber that generally develops during rolling processes [33]. After annealing at 300 °C, the strength of the Brass component decreases and it evolves into the {011}⟨111⟩ α_{fcc}-fiber component, and the {011}⟨111⟩ component becomes dominant in the case of 400 °C. As the temperature further increases to 500 °C, the dense {112}⟨131⟩ component and recrystallized texture {001}⟨100⟩ component are found. This is a typical process to optimize the microstructure of metals. A typical rolling texture is formed after metals are rolled and deformed. Recrystallization reflects the formation of new structures of the deformed metals under heat treatment conditions.

Similarly, a large number of texture components parallel to the RD are generated in the Al matrix of the as-received specimen, including {111}//RD, {110}//RD and {100}//RD, which are concentrated in the LDZ. The intensity of {011}⟨111⟩ α_{fcc}-fiber component decreases and evolves into {001}⟨100⟩ cube texture. As the annealing temperature rises, new slip systems, such as {001}⟨110⟩ slip system, may appear in the Al matrix, which helps to improve the plasticity of the material [34].

5 Conclusions

(1) The thickness of IMCs layer in the specimen annealed at 300 °C does not increase significantly. Obvious IMC layer comprising three sublayers with a thickness of 5 μm is formed in the

specimen annealed at 400 °C, and even 12 μm of the specimen annealed at 500 °C. Additionally, the thickness of diffusion layer is found to be uniform and continuously distributed.

(2) There are a lot of typical rolling texture components in the as-received specimens, including the {025}⟨100⟩ component in Cu matrix and the {011}⟨111⟩ α_{fcc}-fiber component in Al matrix. When the annealing process is completed, recrystallized textures appear in the matrixes, including the {001}⟨100⟩ and {001}⟨110⟩ components, which improve the plasticity of the material.

(3) The ultimate tensile strength of the specimen annealed at 300 °C is slightly lower than that of the as-received specimen. With increasing the annealing temperature from 300 to 500 °C, a dramatic decrease of ultimate tensile strength and a great increase of elongation are observed.

Acknowledgments

This research was supported by the National Natural Science Foundation of China (Nos. 51975398, 51905372), the Fund for Shanxi "1331 Project", China, and the 111 Project, China (No. D21003).

References

[1] SZCZEPANIK S, SLEBODA T. The influence of the hot deformation and heat treatment on the properties of P/M Al−Cu composites [J]. Journal of Materials Processing Technology, 1996, 60: 729−733.

[2] HENESS G, WUHRER R, YEUNG W Y. Interfacial strength development of roll-bonded aluminium/copper metal laminates [J]. Materials Science and Engineering A, 2008, 483/484: 740−742.

[3] YOUSEFI MEHR V, TOROGHINEJAD M R, REZAEIAN A. Mechanical properties and microstructure evolutions of multilayered Al−Cu composites produced by accumulative roll bonding process and subsequent annealing [J]. Materials Science and Engineering A, 2014, 601: 40−47.

[4] PENG X K, WUHRER R, HENESS G, YEUNG W Y. On the interface development and fracture behaviour of roll bonded copper/aluminium metal laminates [J]. Journal of Materials Science, 1999, 34: 2029−2038.

[5] ABBASI M, TAHERI A K, SALEHI M T. Growth rate of intermetallic compounds in Al/Cu bimetal produced by cold roll welding process [J]. Journal of Alloys and Compounds, 2001, 319: 233−241.

[6] SEIFOLLAHZADEH P, ALIZADEH M, ABBASI M R. Strength prediction of multi-layered copper-based composites fabricated by accumulative roll bonding [J]. Transactions of Nonferrous Metals Society of China, 2021, 31: 1729−1739.

[7] ASEMABADI M, SEDIGHI M, HONARPISHEH M. Investigation of cold rolling influence on the mechanical properties of explosive-welded Al/Cu bimetal [J]. Materials Science and Engineering A, 2012, 558: 144−149.

[8] TAVASSOLIMANESH A, ALAVI NIA A. A new approach for manufacturing copper-clad aluminum bimetallic tubes by friction stir welding (FSW) [J]. Journal of Manufacturing Processes, 2017, 30: 374−384.

[9] KHOJASTEHNEZHAD V M, POURASL H H. Microstructural characterization and mechanical properties of aluminum 6061-T6 plates welded with copper insert plate (Al/Cu/Al) using friction stir welding [J]. Transactions of Nonferrous Metals Society of China, 2018, 28: 415−426.

[10] LEE K S, KWON Y N. Solid-state bonding between Al and Cu by vacuum hot pressing [J]. Transactions of Nonferrous Metals Society of China, 2013, 23: 341−346.

[11] GUO Ya-jie, QIAO Guan-jun, JIAN Wen-zheng, ZHI Xiao-hui. Microstructure and tensile behavior of Cu−Al multi-layered composites prepared by plasma activated sintering [J]. Materials Science and Engineering A, 2010, 527: 5234−5240.

[12] KELLER C, MOISY F, NGUYEN N, EVE S, DASHTI A, VIEILLE B, GUILLET A, SAUVAGE X, HUG E. Microstructure and mechanical properties characterization of architectured copper aluminum composites manufactured by cold-drawing [J]. Materials Characterization, 2021, 172: 110824.

[13] HUG E, BELLIDO N. Brittleness study of intermetallic (Cu, Al) layers in copper-clad aluminium thin wires [J]. Materials Science and Engineering A, 2011, 528: 7103−7106.

[14] XU Hui, LIU Chang-qing, SILBERSCHMIDT V V, PRAMANA S S, WHITE T J, CHEN Zhong, ACOFF V L. Behavior of aluminum oxide, intermetallics and voids in Cu−Al wire bonds [J]. Acta Materialia, 2011, 59: 5661–5673.

[15] WANG Jian, MISRA A. An overview of interface-dominated deformation mechanisms in metallic multilayers [J]. Current Opinion in Solid State and Materials Science, 2011, 15: 20−28.

[16] WU Xiao-lei, YANG Mu-xin, YUAN Fu-ping, WU Gui-lin, WEI Yu-jie, HUANG Xiao-hu, ZHU Yun-tian. Heterogeneous lamella structure unites ultrafine-grain strength with coarse-grain ductility [J]. Proceedings of the National Academy of Sciences of the United States of America, 2015, 112: 14501−14505.

[17] MAO Zhi-ping, XIE Jing-pei, WANG Ai-qing, WANG Wen-yan, MA Dou-qin, LIU Pei. Effects of annealing temperature on the interfacial microstructure and bonding strength of Cu/Al clad sheets produced by twin-roll casting and rolling [J]. Journal of Materials Processing Technoloty, 2020, 285: 116804.

[18] SHENG Li-yuan, YANG Fang, XI Ting-fei, LAI Chen, YE Heng-qiang. Influence of heat treatment on interface of Cu/Al bimetal composite fabricated by cold rolling [J]. Composites Part B: Engineering, 2011, 42: 1468−1473.

[19] LI Xiao-bing, ZU Guo-yin, WANG Ping. Asymmetry in interface and bending property of Al/Cu/Al bimetallic laminates [J]. Rare Metals, 2014, 33: 556−562.

[20] LI Xiao-bing, ZU Guo-yin, WANG Ping. High strain rate

tensile performance and microstructural evolution of Al/Cu laminated composite under dynamic loading [J]. Materials Science and Engineering A, 2014, 612: 89−95.
[21] KIM I K, HONG S I. Mechanochemical joining in cold roll-cladding of tri-layered Cu/Al/Cu composite and the interface cracking behavior [J]. Materials & Design, 2014, 57: 625−631.
[22] KIM W N, HONG S I. Interactive deformation and enhanced ductility of tri-layered Cu/Al/Cu clad composite [J]. Materials Science and Engineering A, 2016, 651: 976−986.
[23] TAYYEBI M, RAHMATABADI D, KARIMI A, ADHAMI M, HASHEMI R. Investigation of annealing treatment on the interfacial and mechanical properties of Al5052/Cu multilayered composites subjected to ARB process [J]. Journal of Alloys and Compounds, 2021, 871: 159513.
[24] ASTM E8. ASTM E8/E8M standard test methods for tension testing of metallic materials [S]. 2010.
[25] JATA K V, SEMIATIN S L. Continuous dynamic recrystallization during friction stir welding of high strength aluminum alloys [J]. Scripta Materialia, 2000, 43: 743−749.
[26] CHU Di, ZHANG Jian-yu, YAO Jin-jin, HAN Yan-qiu, WU Chun-jing. Cu−Al interfacial compounds and formation mechanism of copper cladding aluminum composites [J]. Transactions of Nonferrous Metals Society of China, 2017, 27: 2521−2528.
[27] ZHAO Jing-wei, HUO Ming-shuai, MA Xiao-guang, JIA Fang-hui, JIANG Zheng-yi. Study on edge cracking of copper foils in micro rolling [J]. Materials Science and Engineering A, 2019, 747: 53−62.
[28] SKROTZKI W, SCHEERBAUM N, OERTEL C G, ARRUFFAT-MASSION R, SUWAS S, TÓTH L S. Microstructure and texture gradient in copper deformed by equal channel angular pressing [J]. Acta Materialia, 2007, 55: 2013−2024.
[29] HUMPHREYS F J, HATHERLY M. Grain growth following recrystallization [M]//Recrystallization and Related Annealing Phenomena. Amsterdam: Elsevier, 2004, 333−378.
[30] PETCH N J. The cleavage strength of polycrystals [J]. J Iron Steel InstInst, 1953, 174: 25−28.
[31] MEYERS M A, MISHRA A, BENSON D J. Mechanical properties of nanocrystalline materials [J]. Progress in Materials Science, 2006, 51: 427−556.
[32] MAO Wei-min. Intergranular mechanical equilibrium during the rolling deformation of polycrystalline metals based on Taylor principles [J]. Materials Science and Engineering A, 2016, 672: 129−134.
[33] DELANNAY L, MISHIN O V, JENSEN D J, VAN HOUTTE P. Quantitative analysis of grain subdivision in cold rolled aluminium [J]. Acta Materialia, 2001, 49: 2441−2451.
[34] ZHANG Ning, YANG Ping, MAO Wei-min. {001}⟨120⟩-{113}⟨361⟩ recrystallization textures induced by initial {001} grains and related microstructure evolution in heavily rolled electrical steel [J]. Materials Characterization, 2016, 119: 225−232.

退火温度对铜/铝复合薄带组织和拉伸性能的影响

王 琛[1,2,3]，马丽楠[4]，马晓光[1,2,3]，王 涛[1,2,3]，姜正义[5,6]，Mahadi HASAN[7]，赵敬伟[1,2,3]

1. 太原理工大学 机械与运载工程学院，太原 030024；
2. 先进金属复合材料成形技术与装备教育部工程研究中心，太原 030024；
3. 太原理工大学 中澳联合研究中心，太原 030024；
4. 太原科技大学 机械工程学院，太原 030024；
5. School of Mechanical, Materials, Biomedical and Mechatronic Engineering, University of Wollongong, NSW 2522, Australia;
6. TYUT-UOW Joint Research Center, University of Wollongong, NSW 2522, Australia;
7. Department of Industrial and Production Engineering, American International University Bangladesh, Dhaka 1229, Bangladesh

摘 要：研究退火温度对铜/铝(Cu/Al)复合薄带的组织和拉伸性能的影响以提高材料的力学性能。使用扫描电子显微镜(SEM)、能谱仪(EDS)和电子背散射衍射仪(EBSD)观察和分析界面层的变化、界面元素的扩散以及 Cu 和 Al 各基体的显微组织演变。通过静态单轴拉伸试验研究 Cu/Al 复合薄带的拉伸性能。结果表明，Cu/Al 基体在退火过程中发生再结晶，在 400 ℃退火后 Al 基体晶粒生长成粗大晶粒。扩散层厚度随着退火温度的升高而增加，500 ℃退火后扩散层厚度达到 12 μm。原始典型轧制织构经退火处理后转变为典型退火织构成分{001}⟨100⟩和{001}⟨110⟩。一般来说，退火处理降低了材料的抗拉强度，提高了材料的整体塑性，扩散层在传递拉应力方面起着显著作用。

关键词：铜/铝复合材料；退火处理；显微组织；织构；拉伸性能

(Edited by Xiang-qun LI)